Electronic supplementary information

Enhancement of Magnetic Heating Efficiency in Size Controlled MFe_2O_4 (M = Mn, Fe, Co and Ni) Nanoassemblies

Jeotikanta Mohapatra,[a] Saumya Nigam,[b] J. Gupta,[c] A. Mitra,[d] M. Aslam,[a,d,*] D. Bahadur,[a,c,*]

[a]Centre for Research in Nanotechnology and Science (CRNTS), [b]IITB-Monash Research Academy, [c]Department of Metallurgical Engineering and Materials Science, [d]Department of Physics, Indian Institute of Technology Bombay, Powai, Mumbai-40076, India

**To whom correspondence should be addressed.* *m.aslam@iitb.ac.in*. (M. Aslam). *Phone: +91 22 2576 7585, E-mail: dhirenb@iitb.ac.in*. (D. Bahadur), *Phone: +91 22 2576 7632*

(A) Experimental Technique

X-ray diffraction (XRD) spectra were retrieved from Xpert PANAlytic X-ray diffractometer with Cu Kα radiation (λ = 1.54 Å). FTIR spectra were taken on Bruker, Vertex-80 using KBr pellet. High-resolution transmission electron microscopy images and selected area diffraction patterns were obtained with JEOL JEM 2100F, field emission gun transmission electron microscope (FEG-TEM*)* at an accelerating voltage of 200 kV. The scanning electron micrographs (SEM) were taken by JSM-7600F FEG SEM. Thermogravimetric analysis (TGA) of coated Fe_3O_4 MNNAs was carried out using a Perkin-Elmer Pyris instrument. TGA measurements were made from room temperature to 600 °C with a heating rate of 10 °C/min. The surface area and porosity measurements were performed by Micromeritics ASAP 2020 surface area and porosity analyzer. These samples were degassed at 90 °C for 2 h and then at 200 °C for 4 h by surface area and porosity analyzer prior to surface area, pore volume and pore size measurements. The ζ-potential measurements were carried out by the Zetasizer nano series, Malvern Instruments. The magnetic properties of the samples were studied using physical property measurement system (Quantum Design PPMS). The isothermal magnetization (M) versus applied magnetic field (H), zero-field-cooled (ZFC), and field-cooled (FC) measurements were performed over the temperature range 10–300 K with applied field of 20 kOe. The applied external field for ZFC and FC isotherm was 200 Oe.

(B) Synthesis of 4-24 nm Fe_3O_4 nanoparticles

Uniform Fe_3O_4 nanoparticles ($\sigma \leq 15\%$) are prepared using our previously published protocol.[1] In a typical synthesis of 4 nm Fe_3O_4 nanoparticles, a mixture of 4 mM of $FeCl_2$ and 28 mM of oleylamine (precursor to amine molar ratio 1:7) was heated at 200 ˚C under N_2 atmosphere. The size was controlled with the molar ratio of precursor to amine as 1:3 (9 nm) and 1:5 (6 nm), respectively. To further increase the particle size above 9 nm, a seed-mediated growth model was utilized.

(C) Theoretical basis of magnetic fluid heating

The principal equations of SAR and the power dissipation (P) are as follows.[2, 3]

$$SAR = \frac{P}{\rho\varphi} \quad \text{..... (1)}$$

$$P = \Delta U f = \mu_0 \pi H_0^2 \chi'' f \quad \text{..... (2)}$$

where ρ the density of magnetic material, φ the volume fraction of nanoparticles in the suspension, μ_0 the magnetic permeability, H_0 the magnetic field, $\omega = 2\pi f$ the frequency of the applied ACMF.

The frequency dependence of the complex susceptibility (χ'') is expressed as follows.

$$\chi'' = \frac{\mu_0 V M_S^2}{3\phi k_B T} \frac{\omega\tau}{1+(\omega\tau)^2} \quad \text{..... (3)}$$

where M_S is the saturation magnetization, V is the volume of the nanoparticle and τ is the effective relaxation time which is consisted of Brownian (τ_B) and Néel (τ_N) relaxation time. This relaxation times are as follows

$$\tau_B = \frac{3\eta V_H}{k_B T} \quad \text{..... (4)}$$

$$\tau_N = \frac{M_S}{2\gamma_0 K_{eff}^{3/2}} \left(\frac{\pi k_B T}{V}\right)^{1/2} \exp\left(\frac{K_{eff} V}{k_B T}\right) \quad \text{..... (5)}$$

Where η = viscosity coefficient of the matrix fluid, k_B = Boltzmann constant, T = absolute temperature, V_H = hydrodynamic volume and K_{eff} = effective anisotropy constant. Because the Brownian and Néel processes take place in parallel, the effective relaxation time τ is given by

$$\frac{1}{\tau} = \frac{1}{\tau_B} + \frac{1}{\tau_N} \text{ …..... (6)}$$

In superparamagnetic regime the Brownian contribution can be neglected, $\tau = \tau_N$.

Hence, $\tau = \frac{M_S}{2\gamma_0 K_{eff}^{3/2}} \left(\frac{\pi k_B T}{V} \right)^{1/2} \exp\left(\frac{K_{eff} V}{k_B T} \right)$ …..... (7)

From equation 2, 3 and 7, it is clear that the maximum power loss is directly related to the M_S and complex susceptibility (χ''). The M_S value of a material can be tuned by controlling the nanocrystals size and composition. The χ'' has a maximum value at $\omega\tau_N=1$. Further, the Néel relaxation time is exponentially dependent on the product of K_{eff} and V; therefore, in material with higher K_{eff}, the particle size which satisfies the maximum loss condition shifts to lower nanocrystals size. The critical size corresponding to maximum heating is found to be 6, 15 and 27 nm for $CoFe_2O_4$, Fe_3O_4 and $MnFe_2O_4$ nanocrystals respectively.

Further the relationship between critical nanoparticles volume corresponding to maximum heating ($\omega\tau_N=1$) can be expressed as

$$\left. \frac{\partial \tau_N}{\partial V} \right]_{V=Vm} = 0$$
$$\Rightarrow Vm = \frac{a}{K_{eff}} \text{ …..... (8)}$$

where a is constant.

(D) Surface functionalization of MFe_2O_4 MNNAs: FTIR study

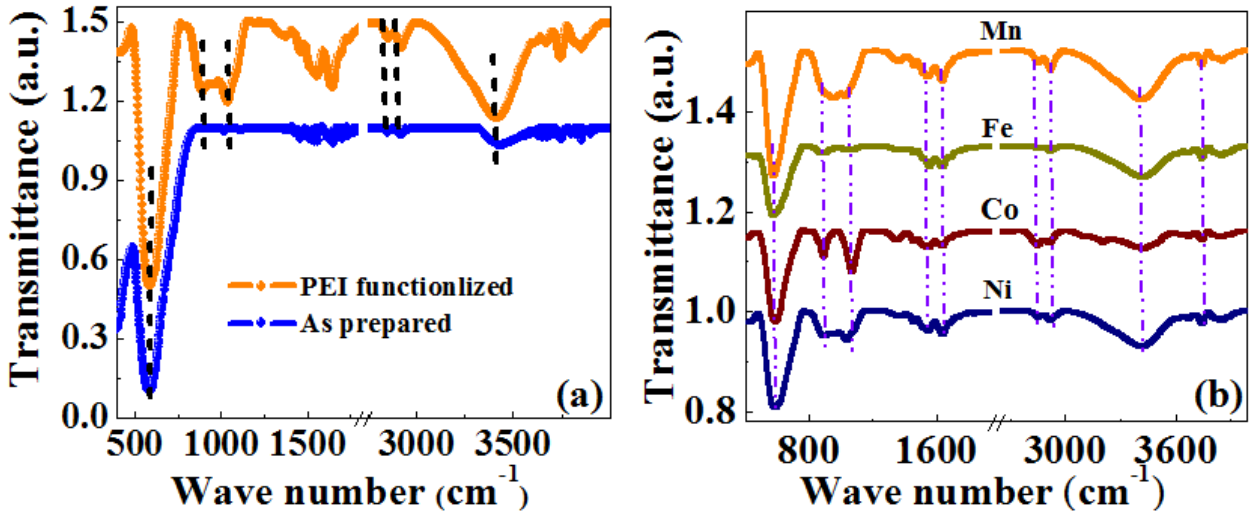

Fig. S1 (a) Represents the FTIR spectra of as prepared and PEI functionalized Fe_3O_4 MNNAs (80 nm). The intensity of amine-related FTIR peaks (N-H stretching mode of primary amine at 3740 cm^{-1} and C-N stretching at 1068 cm^{-1}) in as prepared sample is weak and becomes prominent after surface fictionalization with PEI.[4, 5] It indicates that in the as prepared Fe_3O_4 MNNAs a small amount of PEG-amine functional groups are coordinated to the iron cations, after surface modification there are large amount of PEI molecules located on the particles surface. All these results confirmed that PEI-functionalized Fe_3O_4 MNNAs have been successfully obtained. **(b)** FTIR spectra of PEI-functionalized MFe_2O_4 MNNAs (80 nm). The typical low frequency band at around 578 cm^{-1} refers to Fe-O vibration (Fe^{3+} bond) in octahedral and tetrahedral sites, which could be attributed to spinel ferrite phase of Fe_3O_4 while the Fe-O band for γ- Fe_2O_3 is usually seen at 540 cm^{-1}.[6] The high frequency band at 3740 cm^{-1} is assigned to N-H stretching mode of primary amine, while the C-H bending, C-N stretching, CH_2 scissoring and NH_2 scissoring peaks appear at 895 cm^{-1}, 1068 cm^{-1}, 1546 cm^{-1} and 1645 cm^{-1} respectively.[4, 5] The peaks at 2852 cm^{-1} and 2930 cm^{-1} are assigned to CH_2 vibrations originating from the polyethylenimine. The strong band observed at 3410 cm^{-1} is ascribed to O-H vibration originating from physically adsorbed water molecules.[4]

(E) Crystal structure and morphology

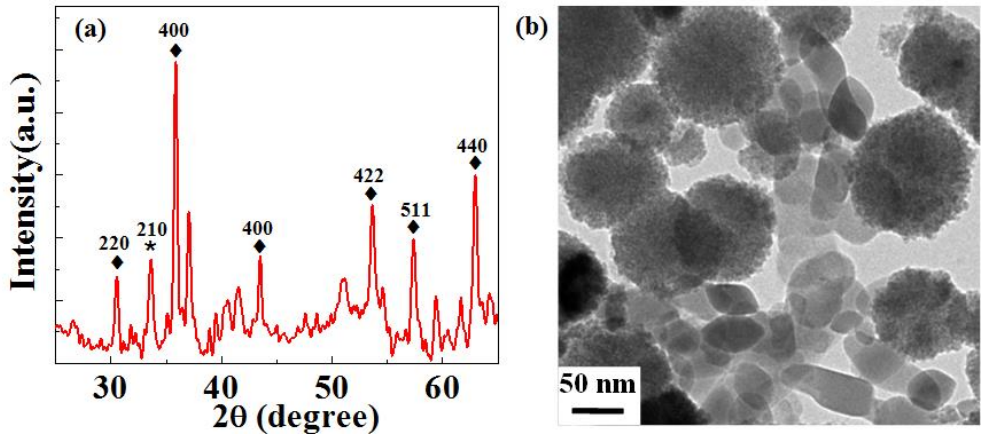

Fig. S2: (a) The XRD spectra of iron oxide nanoparticles produced using 9 mmol Fe-precursor shows mixed phase of Fe_3O_4 (♦) and α- Fe_2O_3 (*). (b) The representative TEM micrograph of the sample produced using 9 mmol Fe-precursor shows non-uniformity in shape as well as size.

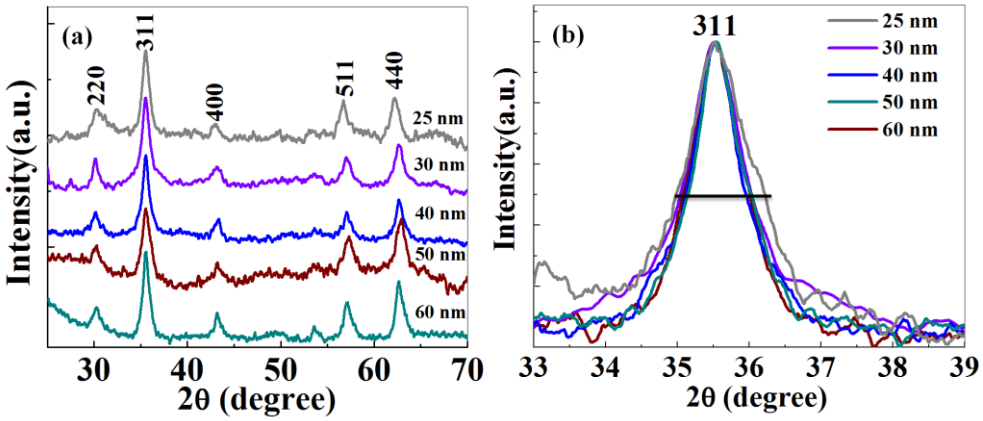

(c)

Assembly size (nm)	Crystallite size (nm)	Lattice strain
25	4 ± 1	1.624
30	4.6 ± 1	1.514
40	4.6 ± 1	1.498
50	4.8 ± 1	1.317
60	5 ± 1	1.277

Fig. S3: (a) XRD spectra of different sized Fe_3O_4 MNNAs prepared using EG as solvent. (b) The full width half maxima (FWHM) and peak position for the entire sample are nearly same. This indicates that the nanocrystal size of the MNNAs prepared using EG is nearly the same. (c) The variation of nanocrystal size and lattice strain with Fe_3O_4 MNNAs size.

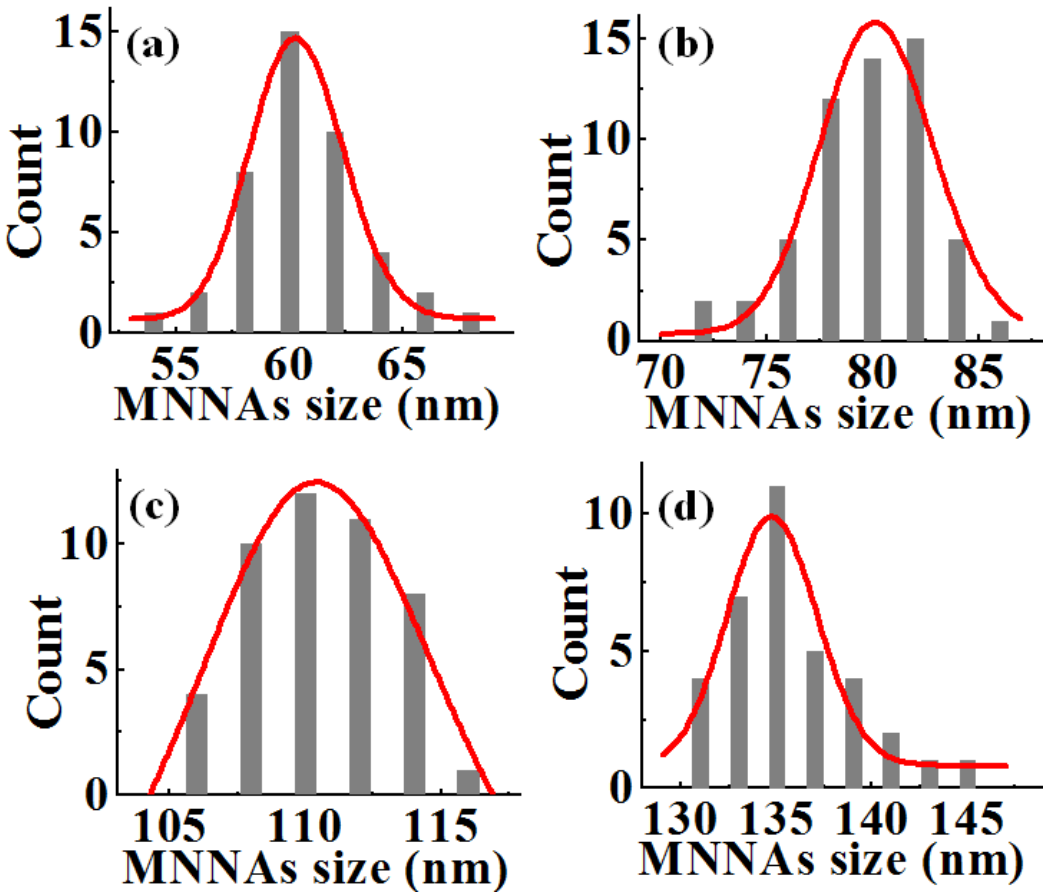

Fig. S4: Histograms of the particle size distribution of Fe_3O_4 MNNAs prepared with the PEG contents of ; (a) 2 ml, (b) 5 ml, (c) 8 ml and (d) 12 ml. The statistical analysis has been done by measuring the size of almost 45-60 particles. The average MNNAs size is estimated from TEM micrograph using the lognormal distribution.

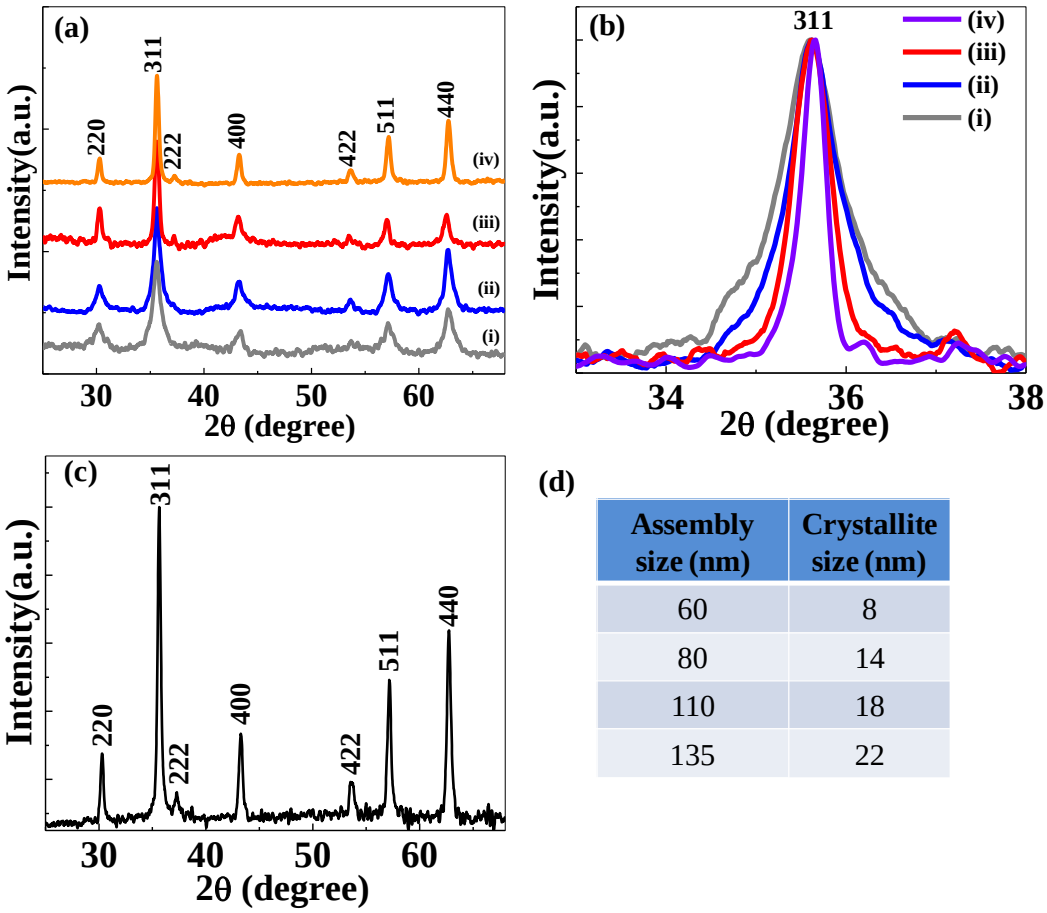

(d)

Assembly size (nm)	Crystallite size (nm)
60	8
80	14
110	18
135	22

Fig. S5: (a) XRD spectra of different size (60 nm –i, 80 nm –ii, 110 nm –iii and 135 nm –iv) Fe_3O_4 MNNAs prepared using EG and PEG as solvent. (b) The full width half maxima (FWHM) increases with the increases of MNNAs size, which indicates that the nanocrystals size of the MNNAs prepared using EG and PEG increases with increases of nanoassemblies size. (c) The XRD spectra of MNNAs produced using 20 ml of PEG shows narrow bordering in the XRD spectrum. (d) Shows the variation of nanocrystals size with Fe_3O_4 MNNAs size.

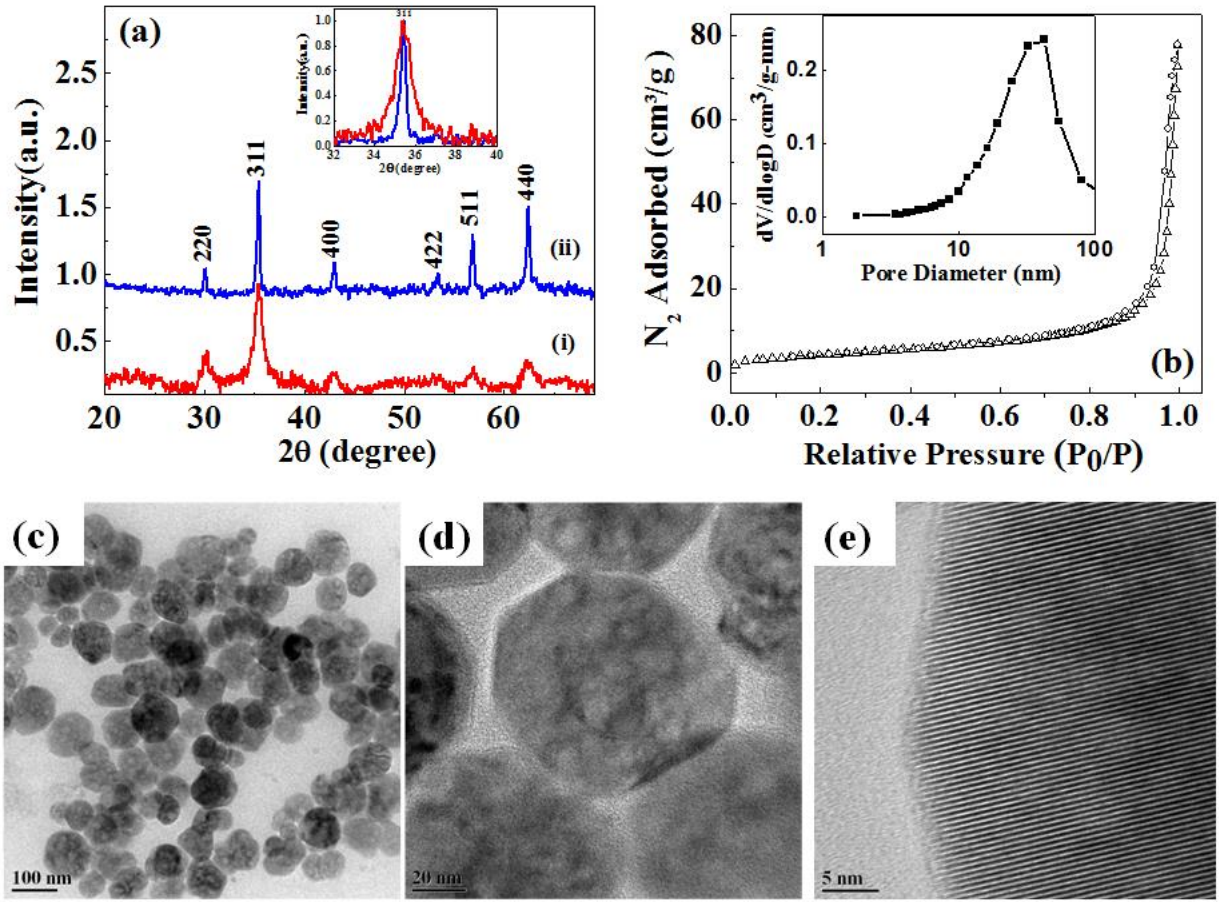

Fig. S6: (a) XRD pattern of Fe_3O_4 nanoparticles produced with the usage of 12 ml PEG (red curve) (i) and 20 ml PEG (blue curve) (ii). Inset shows the narrow broadening in the 311 XRD peak for the sample prepared with 20 ml PEG. (b) Surface area and porosity of 80 nm Fe_3O_4 nanoparticles is determined by measuring the adsorption and desorption isotherms of N_2. The average pore size is 50 nm assigned to the inter-particle distance. (c) TEM and (b) and (c) HR-TEM images of Fe_3O_4 nanoparticles produced with 20 ml of PEG.

(F) Magnetic properties

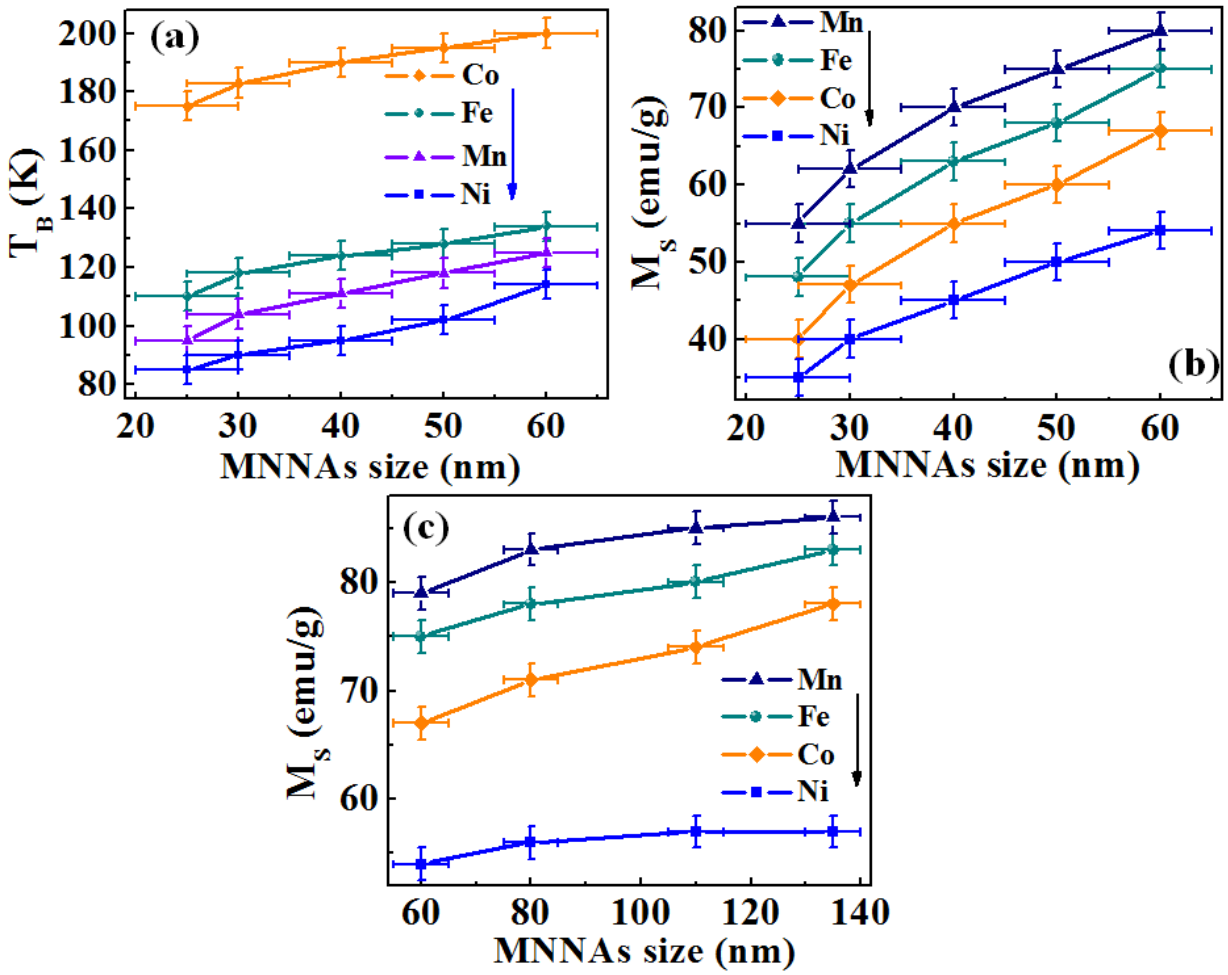

Fig. S7: (a) Blocking temperature vs. MNNA size plot of all MFe_2O_4 (M = Mn, Fe, Co and Ni) MNNAs of size 25-60 nm. The size of the MNNAs is controlled by varying the mole content of metal chloride precursor. Although the nanocrystallite size of 25- 60 nm sized MFe_2O_4 MNNAs are nearly the same, we observed a linear increment of T_B with the nanoassembly size, which could be due to magnetic couplings between the nanocrystals within the MNNA. (b) M_S value vs. MNNA size plot of all MFe_2O_4 MNNAs of size 25-60 nm. M_S value shows an increasing trend with the increase of size of MNNAs. (c) The variation of room temperature M_S value with size of MFe_2O_4 MNNAs ($\sigma \leq 20$ %) prepared by using bisolvent mixture of EG and PEG.

(G) Hyperthermia characteristics

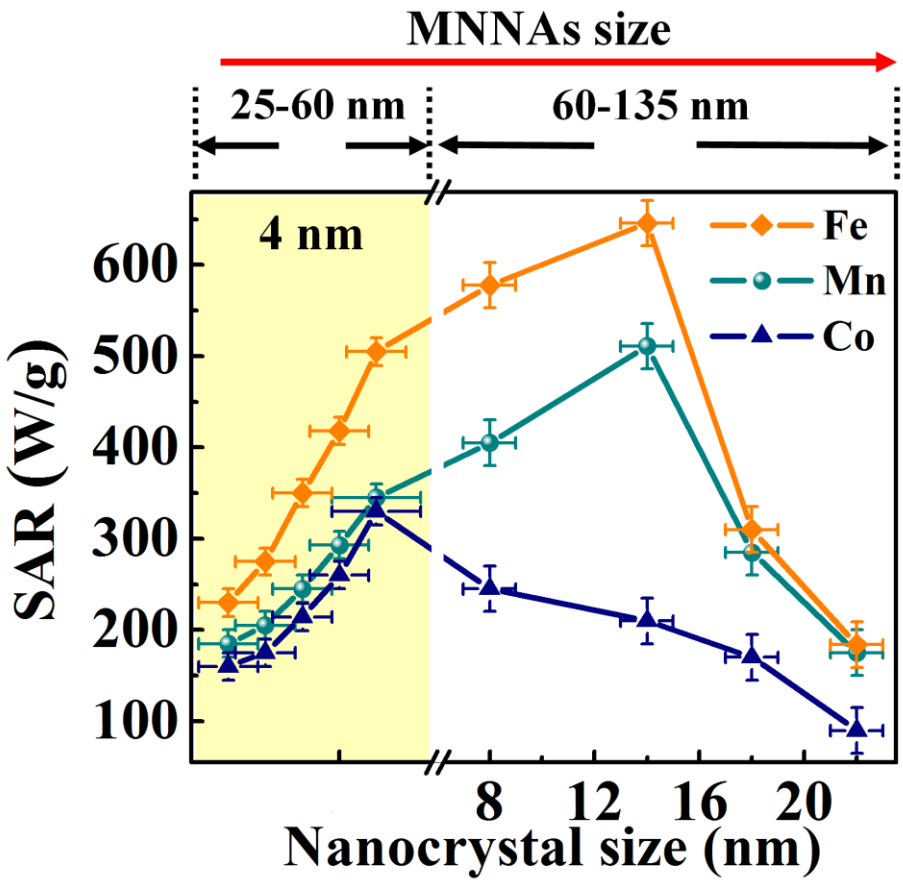

Fig. S8: Demonstrates an optimization of heat activation efficiency of MFe_2O_4 nanocrystals nanoassemblies (MNNAs) by controlling size, composition and magnetic coupling among the nanocrystals within the MNNAs. The highlighted part (yellow) represents the SAR results of similar nanocrystallite sized MFe_2O_4 MNNAs and the SAR values are controlled by varying the MNNAs size from 25-60 nm. The increase in SAR values with MNNAs size (of similar nanocrystallite size) is due to the magnetic coupling between the nanocrystals with the nanoassembly. To further improve the SAR value, the size of the nanocrystals (8-22 nm) as well as MNNAs (60-135 nm) is controlled by using bi-solvent mixture of PEG and EG. The non-highlighted part of the figure shows the SAR values for 60-135 nm sized MFe_2O_4 MNNAs. Here, the SAR values are controlled by varying both the nanocrystals and nanoassembly size to achieve a high efficiency magnetic heating material.

(H) Elemental composition analysis

Table S1: Elemental composition of 110 nm sized MFe_2O_4MNNAs measured by EDX and ICP-AES.

Sample Code	Fe atom (%)		M atom (%)		Fe/M ratio	
	EDX	ICP-AES	EDX	ICP-AES	EDX	ICP-AES
$MnFe_2O_4$	28.4	29.2	13.1	14.2	2.1	2
$CoFe_2O_4$	26.2	26.8	11.3	12.8	2.3	2.3
$NiFe_2O_4$	25.9	27.4	13.7	13.5	1.9	2

References:

1. J. Mohapatra, A. Mitra, D. Bahadur and M. Aslam, *CrystEngComm*, 2013, **15**, 524-532.
2. R. E. Rosensweig, *J. Magn. Magn. Mater.*, 2002, **252**, 370-374.
3. J. Carrey, B. Mehdaoui and M. Respaud, *J. Appl. Phys.*, 2011, **109**, 083921.
4. P. Griffiths and J. A. De Haseth, *Fourier transform infrared spectrometry*, Wiley-Interscience, 2007.
5. M. Chen, Y.-G. Feng, X. Wang, T.-C. Li, J.-Y. Zhang and D.-J. Qian, *Langmuir*, 2007, **23**, 5296-5304.
6. Z. Xu, C. Shen, Y. Hou, H. Gao and S. Sun, *Chem. Mater.*, 2009, **21**, 1778-1780.